Int J CARS (2012) 7:359–369
DOI 10.1007/s11548-011-0626-9

ORIGINAL ARTICLE

Real-time marker-free patient registration for electromagnetic navigated bronchoscopy: a phantom study

Daisuke Deguchi · Marco Feuerstein · Takayuki Kitasaka · Yasuhito Suenaga · Ichiro Ide · Hiroshi Murase · Kazuyoshi Imaizumi · Yoshinori Hasegawa · Kensaku Mori

Received: 25 January 2011 / Accepted: 20 May 2011 / Published online: 7 June 2011

Abstract
Purpose To perform bronchoscopy safely and smoothly, it is very important to develop a bronchoscopic guidance system. Transbronchial lung biopsy (TBLB) with a bronchoscopic guidance system especially should permit safe image-guided procedures. Recently, electromagnetic tracking (EMT) is utilized to track the tip of the bronchoscope camera in real time. For most tracking methods using position sensors, registration between tracking data and previously acquired reference image data, such as CT image, is performed using natural landmarks of the patient or fiducial markers attached to the patient, whose positions need to be measured manually by the physician before the actual bronchoscopy. Therefore, this paper proposes a marker-free CT-to-patient registration method utilizing bronchoscope's position and orientation obtained by the EMT.
Methods We developed a guidance system that is able to track the tip of the bronchoscope camera in real time. In the case of a guidance system that uses position sensors, natural landmarks of the patient or fiducial markers attached to the patient are needed to obtain the correspondence between EMT outputs and previously acquired reference image data, such as CT image. This paper proposes a registration method without landmarks or fiducials by estimating the transformation matrix between the patient and the CT image taken prior to the bronchoscopic examination. This estimation is performed by computing correspondences between the outputs of the EMT sensor and airways extracted from the CT image. As ambiguities between EMT measurements and their corresponding airway branches may arise at airway bifurcations, we introduce a stable airway branch selection mechanism for improving the robustness of the estimation of the transformation matrix. To evaluate the performance of the proposed method, we applied the method to a rubber bronchial phantom and added virtual breathing motion to the sensor output.
Results Experimental results show that the accuracy of our proposed method is within $2.0-3.0$ mm (without breathing motion) and $2.5-3.5$ mm (with breathing motion). The proposed method could also track a bronchoscope camera in real time.
Conclusions We developed a method for CT-to-patient registration using a position sensor without fiducial markers and natural landmarks. Endoscopic guided biopsy of lung lesions is feasible using a marker-free CT-to-patient registration method.

Keywords Bronchoscopy · Virtual bronchoscopy · Position sensor · Marker-free registration · Motion recovery · Tracking · Camera tracking

D. Deguchi (✉) · M. Feuerstein · I. Ide · H. Murase · K. Mori
Graduate School of Information Science, Nagoya University,
Furo–cho, Chikusa–ku, Nagoya–shi, Aichi 464–8601, Japan
e-mail: ddeguchi@is.nagoya-u.ac.jp

M. Feuerstein
Fakultät für Informatik, Technische Universität München,
Boltzmannstr. 3, 85748 Garching, Germany

T. Kitasaka · Y. Suenaga
Faculty of Management and Information Science,
Aichi Institute of Technology, 1247 Yachigusa,
Yakusa–cho, Toyota–shi, Aichi 470–0392, Japan

K. Imaizumi · Y. Hasegawa
Graduate School of Medicine, Nagoya University,
65 Tsurumai–cho, Showa–ku, Nagoya–shi,
Aichi 466–8550, Japan

Introduction

A bronchoscope is a very important tool for diagnosis of the airways or performing biopsies of suspicious regions. In recent years, ultra-thin bronchoscopes have become

commercially available, which allow a physician to insert it into narrower bronchial branches. In the case of transbronchial lung biopsy (TBLB), a physician needs to move the bronchoscope through many branches and furcations, before a biopsy can be performed. However, a physician performs bronchoscope insertion by only using bronchoscopic images and his/her knowledge. In addition, the airways have a very complex tree structure with similar bifurcation patterns. Therefore, a physician may be easily confused and lose the way to the target region. Moreover, blood vessels behind the bronchial wall cannot be seen in a bronchoscopic image. To solve these problems, it is important to develop a bronchoscopic guidance system which supports a physician by giving the following useful information: (1) current location of the bronchoscope, (2) anatomical structures located behind the bronchial wall, (3) anatomical names of branches currently observed, and (4) paths to the desired location where the biopsy should be performed.

As shown in Fig. 1, a bronchoscopic guidance system combines images from a real bronchoscope and a virtual bronchoscope [1–7] to provide valuable information, such as anatomy and structures only visible in CT, that would allow the physician to operate the bronchoscope smoothly in compliance with a planned path and in real time. This system should have two fundamental functions: (a) continuous tracking of the bronchoscope tip and (b) display of navigation information. In particular, (a) is a crucial function because most guidance information is generated from the camera position.

Several research groups have proposed methods for tracking a bronchoscope. These methods are categorized as (i) methods based on image registration techniques [8–11], and (ii) methods using electromagnetic tracking (EMT) [12–14,16]. Most methods using image registration track the bronchoscope by comparing a real bronchoscopic image with virtual bronchoscopic images generated from a CT image taken prior to the bronchoscopy. Bricault et al. [8] calculated the bronchoscope camera position using bifurcation information. Mori et al. [11] employed epipolar geometry analysis for avoiding local minima in the image registration step. Higgins et al. proposed a method for tracking a camera using mutual information [9], and they improved their method by introducing 2D/2D matching frameworks to obtain 3D camera motion [10]. These methods are robust against breathing or cardiac motion; however, it is difficult to track quick movements or to recover the tracking process after tracking fails once. Also, since many real and virtual bronchoscopic images need to be compared in the image registration process, it is difficult to track the camera pose in real time.

In recent years, EMT is becoming a useful tool to track the position and the orientation of surgical tools. Also, an ultra tiny EMT sensor with a diameter of less than 2 mm has become commercially available. Since it can be inserted into the working channel of a typical bronchoscope, some research groups use EMT for tracking the bronchoscope camera. Schneider et al. used outputs of such an EMT sensor for tracking the camera [12]. They obtained a registration error of 4 mm in the trachea; however, the registration error of thinner branches was still large, e.g., 15 mm in the right upper lobe bronchus. Wegner et al. proposed a method for tracking the camera by mapping EMT outputs onto the medial line of the airways extracted from previously acquired CT images [14]. However, these methods use natural or artificial landmarks (e.g., bifurcation points, fiducial markers) for obtaining the relationship between the coordinate systems of the actual patient and the reference images used for navigation such as CT data. Since they usually require manual interaction for obtaining the positions of landmarks on the patient and in the reference image, they require an additional task for physicians before bronchoscopy. Therefore, it is very important to develop a marker-free algorithm to obtain the relationship between the coordinate systems of the patient and the reference image. In the case of bronchoscopy, we can acquire EMT data very easily because all major branches are checked first during a standard bronchoscopy. Based on this characteristic, our group and Klein et al. proposed a method of CT-to-patient registration without natural landmarks and fiducial markers for bronchoscope camera tracking [15–17]. However, [15] required many EMT outputs at initialization stage, and it took much computation time to perform the registration. In contrast, our method requires only a small number of EMT outputs at initialization stage [16], and we confirmed the effectiveness of the method in different environments [17]. However, [16,17] failed to compute the transformation matrix accurately due to an ambiguity of branch selection when the camera is located around bifurcation points. To solve this problem, this paper proposes a stable airway branch selection mechanism for improving the robustness of the estimation of the transformation matrix. First, the proposed method segments the airways from a CT image taken prior to bronchoscopy, and then the transformation matrix between the respective coordinate systems is computed by matching the outputs of the EMT sensor with the medial line of the extracted airways. This matching process is performed by introducing an approach similar to the iterative closest point (ICP) algorithm [19] with the stable airway branch selection mechanism. Since the proposed method only uses outputs of the EMT sensor to compute the transformation matrix between the coordinate systems, no natural landmarks nor fiducial markers are required.

Our paper is organized as follows. Section "Definition of the coordinate systems" gives some definitions used in this paper. Section "Methods" introduces the proposed method. Section "Experimental results" shows our experimental environment and the results of the evaluation of the proposed method. Finally, we will discuss the results of the proposed

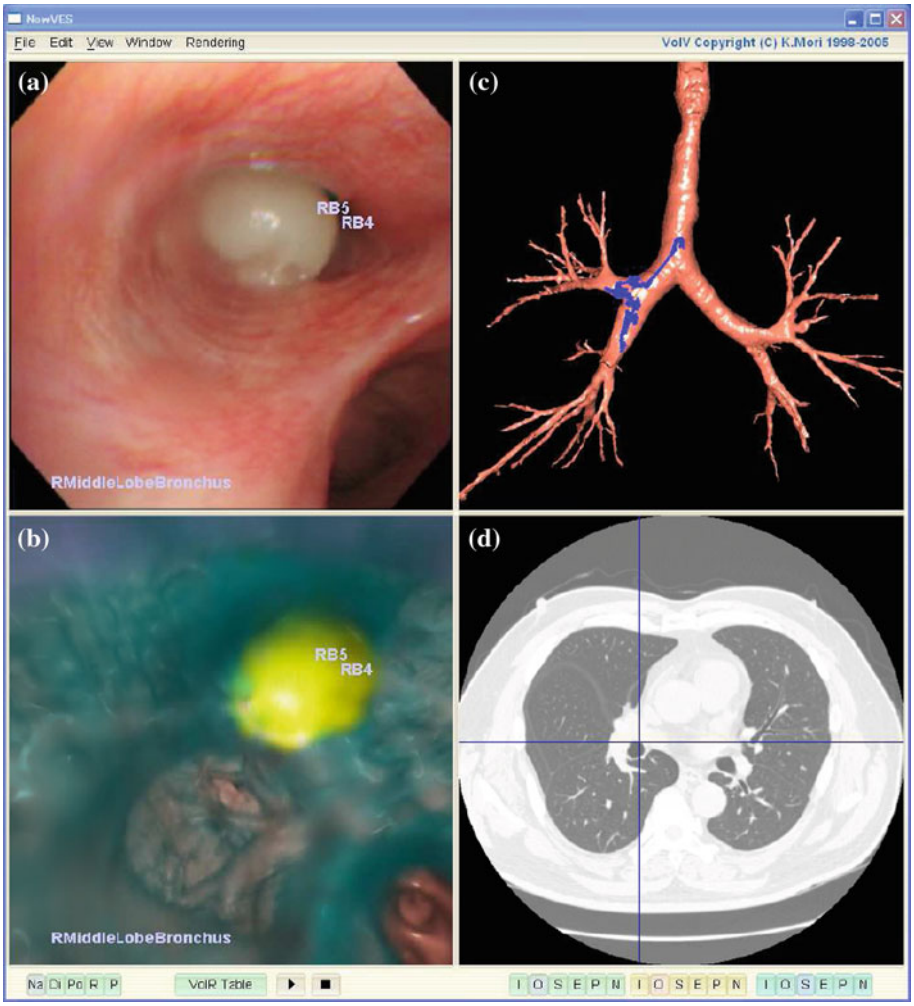

Fig. 1 Example of a bronchoscopic navigation system. This system consists of four windows: **a** a real bronchoscopic video, **b** a virtual bronchoscopic view corresponding to **a**, **c** an outside (bird's eye) view of the airways, and **d** an axial slice image corresponding to the current location of the bronchoscope. Current bronchial branch names are overlaid onto **a**, and anatomical structures behind the bronchus wall can be seen in **b**. Here, the bronchus wall is painted in semi-translucent light blue, and the tumor in yellow. The path of the bronchoscope is shown as a *blue line* on **c**, and the current camera position is marked with a crosscursor in **d**. The information of all windows is synchronized to the current position and orientation of the bronchoscope

method in section "Discussion". This paper is an extended version of the paper presented in MICCAI 2008 [18]. From the MICCAI 2008 paper, we revised algorithm, and detailed experiments and discussions are explained, especially for the effectiveness of the proposed algorithm and for an experiment against virtual breathing motion.

Definition of the coordinate systems

Figure 2 illustrates the relationships and transformation matrices between all coordinate systems used in this paper. We describe the bronchoscope camera positions in the camera coordinate system C and in the CT coordinate system as $\boldsymbol{p}_C$ and $\boldsymbol{p}_{\mathrm{CT}}$, respectively. To also consider patient movement, a dynamic reference frame (DRF) is introduced and defined by a position sensor attached to the patient. In this paper, the DRF is considered as the world coordinate system W, and the bronchoscope camera position in the world coordinate system W is written as $\boldsymbol{p}_W$. From the relations between all coordinate systems shown in Fig. 2, a bronchoscope camera coordinate $\boldsymbol{p}_C$ is transformed into $\boldsymbol{p}_{\mathrm{CT}}$ as

$$\begin{aligned}\boldsymbol{p}_{\mathrm{CT}} &= {}^{\mathrm{CT}}_{W}\mathbf{T}\,{}^{W}_{F}\mathbf{T}\,{}^{F}_{S}\mathbf{T}^{k}\,{}^{S}_{C}\mathbf{T}\,\boldsymbol{p}_C \\ &= {}^{\mathrm{CT}}_{W}\mathbf{T}\,{}^{W}_{S}\mathbf{T}^{k}\,{}^{S}_{C}\mathbf{T}\,\boldsymbol{p}_C \\ &= {}^{\mathrm{CT}}_{W}\mathbf{T}\begin{pmatrix} {}^{W}_{S}\mathbf{R}^{k} & {}^{W}_{S}\boldsymbol{t}^{k} \\ \mathbf{0}^{T} & 1 \end{pmatrix}{}^{S}_{C}\mathbf{T}\,\boldsymbol{p}_C \\ &= {}^{\mathrm{CT}}_{W}\mathbf{T}\,\boldsymbol{p}^{k}_{W}, \end{aligned} \tag{1}$$

where the sensor coordinate system S indicates a coordinate system defined by the EMT sensor attached to the tip of the

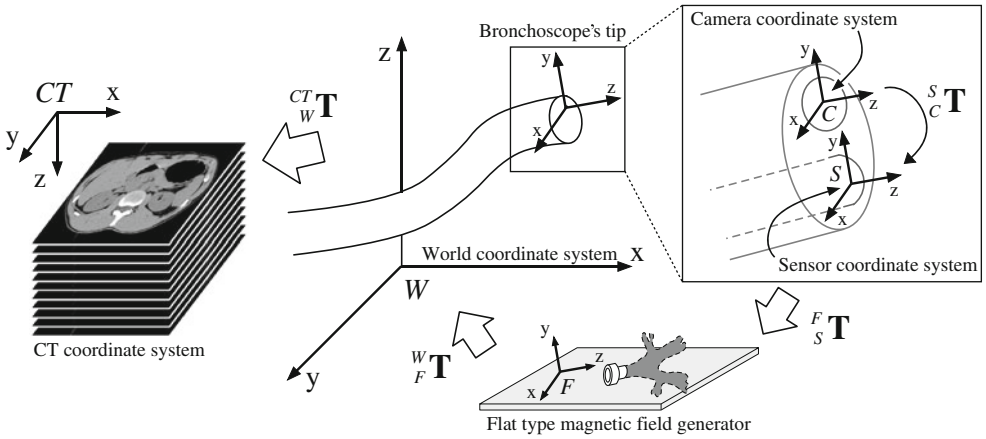

Fig. 2 Relationships between coordinate systems of the bronchoscope camera and the CT image

bronchoscope camera and ${}^{S}_{C}\mathbf{T}$ is the transformation matrix from C to S. The coordinate system of the EMT field generator is represented as F. The transformation matrix ${}^{W}_{F}\mathbf{T}$ is the transformation between the EMT coordinate system F and the world coordinate system W, and ${}^{\mathrm{CT}}_{W}\mathbf{T}$ is the transformation matrix between the world coordinate system W and the CT coordinate system.

It is possible to compute the transformation matrix between the sensor coordinate system S and the world coordinate system W using an EMT sensor output as ${}^{W}_{S}\mathbf{T}^{k} = {}^{W}_{F}\mathbf{T}\,{}^{F}_{S}\mathbf{T}^{k}$, where ${}^{F}_{S}\mathbf{T}^{k}$ is the k-th EMT sensor output. ${}^{W}_{S}\mathbf{R}^{k}$ and ${}^{W}_{S}\boldsymbol{t}^{k}$ are the rotation matrix and the translation vector of the EMT sensor, respectively. ${}^{S}_{C}\mathbf{T}$ shows the relationship between the bronchoscope camera and the EMT sensor and can be obtained when the EMT sensor is attached to the tip of the bronchoscope camera (e.g., by manual or hand–eye calibration [20]). The position and orientation of the bronchoscope camera in the world coordinate system W can be calculated using the outputs of the EMT sensor and ${}^{S}_{C}\mathbf{T}$. Since most navigation or guidance information is generated using virtual bronchoscope camera positions and orientations (represented in the CT coordinate system) corresponding to those of the bronchoscope camera, it is necessary to calculate the transformation matrix ${}^{\mathrm{CT}}_{W}\mathbf{T}$ to obtain the position and orientation of the bronchoscope camera in the CT coordinate system. Therefore, we propose a method for calculating ${}^{\mathrm{CT}}_{W}\mathbf{T}$ that describes the relation between the CT and the DRF attached to the patient and hence allows us to determine the relation between the real bronchoscope and the virtual bronchoscope camera positions and orientations. Since this is a process that computes the mapping between the CT and a real patient, we call this "CT-to-Patient registration" in this paper.

In this paper, the airways and their bronchial tree structure are used for calculating the transformation matrix ${}^{\mathrm{CT}}_{W}\mathbf{T}$, and these data are extracted from the CT image taken prior to bronchoscopy. In the following sections, the i-th bronchial branch $\mathbf{b}_i$ is indicated as $\mathbf{b}_i = \left\{\boldsymbol{b}_i^s, \boldsymbol{b}_i^e\right\}$, where $\boldsymbol{b}_i^s$ and $\boldsymbol{b}_i^e$ are the start and the end positions of $\mathbf{b}_i$ in the CT coordinate system. A set of bronchial branches is indicated as $\mathcal{B} = \{\mathbf{b}_i \mid i = 1, \ldots, M\}$, where M is the number of bronchial branches inside the set $\mathcal{B}$.

Methods

Overview

In this paper, we propose a method to perform CT-to-patient registration without natural landmarks and fiducial markers, which we will outline in the following. First, we assume that the bronchoscope camera moves along the medial line of the airways or close to the center of the airway lumen. Then, we compute the transformation matrix between the coordinate systems of the DRF (defined by the position sensor attached to the patient) and a reference CT image. This is performed by matching the outputs of the EMT sensor attached to the bronchoscope with the medial line of the airways. During bronchoscopy, it is possible to insert the bronchoscope camera freely into the patient and estimate the transformation matrix every few seconds.

The proposed method consists of three steps: (a) preprocessing, (b) acquisition of measurements of the tip of the bronchoscope using EMT, and (c) estimation of the transformation matrix ${}^{\mathrm{CT}}_{W}\mathbf{T}$. The following sections describe the detailed procedures of the proposed method.

Preprocessing

The first step of the proposed method is the extraction of the airways and their tree structure from the CT image taken prior

to bronchoscopy. Here, the airways are extracted by applying our previously developed method [22,23] that can simultaneously extract the airways and their medial line. Also, this method gives the tree structure of the bronchial branches during airway extraction. We use the obtained tree structure for the following matching processes.

Acquisition of bronchoscope positions and orientations by EMT

Prior to calculating the transformation matrix ${}^{\mathrm{CT}}_{w}\mathbf{T}$, the proposed method gathers positions $\boldsymbol{p}^k_w$ and viewing directions $\boldsymbol{d}^k_w$ of the bronchoscope via outputs of an EMT sensor attached to the tip of the bronchoscope. Here, $\boldsymbol{p}^k_w$ and $\boldsymbol{d}^k_w$ are the kth EMT sensor outputs represented in the world coordinate system W and calculated using ${}^{w}_{s}\mathbf{T}^k$. The proposed method records $\mathcal{P} = \left\{\left(\boldsymbol{p}^k_w,\, \boldsymbol{d}^k_w\right)\right\}$ $(k = 1, \ldots, N_1)$ while a physician inserts the bronchoscope into several bronchial branches, where N_1 is the number of EMT sensor outputs. Since many $\boldsymbol{p}^k_w$ and $\boldsymbol{d}^k_w$ are obtained during bronchoscopy, the proposed method can estimate the transformation matrix ${}^{\mathrm{CT}}_{w}\mathbf{T}$ whenever N_1 sensor outputs are obtained. This paper defines $\boldsymbol{p}^k_w$ and $\boldsymbol{d}^k_w$ as $\boldsymbol{p}^k_w = \left(p^k_x,\, p^k_y,\, p^k_z,\, 1\right)^T$ and $\boldsymbol{d}^k_w = \left(d^k_x,\, d^k_y,\, d^k_z,\, 0\right)^T$, where p^k_x, p^k_y, p^k_z, d^k_x, d^k_y and d^k_z are coordinates of $\boldsymbol{p}^k_w$ and $\boldsymbol{d}^k_w$ in the world coordinate system W.

Estimation of the transformation matrix ${}^{\mathrm{CT}}_{w}\mathbf{T}$

In this section, we describe the detailed procedures for computing the transformation matrix ${}^{\mathrm{CT}}_{w}\mathbf{T}$. This consists of three steps: (a) selection of bronchial branches, (b) computation of corresponding point pairs between selected branches and EMT sensor outputs, and (c) estimation of the transformation matrix ${}^{\mathrm{CT}}_{w}\mathbf{T}$ by minimizing the distances between point pairs calculated in (b).

Selection of bronchial branches

First of all, the distance D (as shown in Fig. 3) is calculated for all bronchial branches $\mathbf{b}_i \in \mathcal{B}$ as

$$D\left({}^{\mathrm{CT}}_{w}\mathbf{T}\boldsymbol{p}^k_w, \mathbf{b}_i\right) = \begin{cases} \left\|{}^{\mathrm{CT}}_{w}\mathbf{T}\boldsymbol{p}^k_w - \boldsymbol{b}^s_i\right\|^2 & \text{if } \alpha < 0 \\ \left\|{}^{\mathrm{CT}}_{w}\mathbf{T}\boldsymbol{p}^k_w - \boldsymbol{b}^e_i\right\|^2 & \text{if } \alpha > \left\|\boldsymbol{b}^e_i - \boldsymbol{b}^s_i\right\| \\ \left\|{}^{\mathrm{CT}}_{w}\mathbf{T}\boldsymbol{p}^k_w - \boldsymbol{b}^s_i\right\|^2 - \alpha^2 & \text{otherwise} \end{cases}, \tag{2}$$

$$\alpha = \frac{\left({}^{\mathrm{CT}}_{w}\mathbf{T}\boldsymbol{p}^k_w - \boldsymbol{b}^s_i\right)\cdot\left(\boldsymbol{b}^e_i - \boldsymbol{b}^s_i\right)}{\left\|\boldsymbol{b}^e_i - \boldsymbol{b}^s_i\right\|}, \tag{3}$$

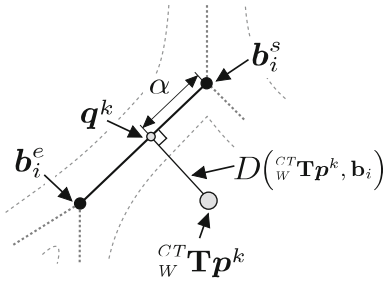

Fig. 3 Relationships between a bronchoscope camera position ${}^{\mathrm{CT}}_{w}\mathbf{T}\boldsymbol{p}^k$ and a bronchial branch $\mathbf{b}_i = \left\{\boldsymbol{b}^s_i, \boldsymbol{b}^e_i\right\}$. $D\left({}^{\mathrm{CT}}_{w}\mathbf{T}\boldsymbol{p}^k, \mathbf{b}_i\right)$ is the distance calculated by Eq. (2), and $\boldsymbol{q}^k$ is the position that corresponds to ${}^{\mathrm{CT}}_{w}\mathbf{T}\boldsymbol{p}^k$

where $\|\ \|$ is the norm of a vector, and $\cdot$ is the inner product of vectors. Then, $\tilde{\mathbf{b}}$ is calculated as

$$\tilde{\mathbf{b}} = \arg\min_{\mathbf{b}_i \in \mathcal{B}} D\left({}^{\mathrm{CT}}_{w}\mathbf{T}\boldsymbol{p}^k_w, \mathbf{b}_i\right). \tag{4}$$

If the bronchoscope is located at bifurcation points of the airways, α calculated by Eq. (3) may be similar for more than one branch. This means that there exists an ambiguity in branch selection. Therefore, the proposed method tries to uniquely determine the correspondences between $\mathbf{b}_*$ and ${}^{\mathrm{CT}}_{w}\mathbf{T}\boldsymbol{p}^k_w$ using the viewing direction $\boldsymbol{d}^k_w$ of the bronchoscope. First, a set of bronchial branches Φ is selected according to Eqs.(3) and (4) as

$$\Phi = \begin{cases} \mathcal{A}(\tilde{\mathbf{b}}) \cup \mathcal{D}(\mathcal{A}(\tilde{\mathbf{b}})) & \text{if } \alpha < \gamma \left\|\tilde{\boldsymbol{b}}^e - \tilde{\boldsymbol{b}}^s\right\| \\ \{\tilde{\mathbf{b}}\} & \text{otherwise} \end{cases}, \tag{5}$$

where $\cup$ represents the set union, γ is a threshold to determine whether ${}^{\mathrm{CT}}_{w}\mathbf{T}\boldsymbol{p}^k_w$ is close to bifurcations, and $\mathcal{A}(\tilde{\mathbf{b}})$ represents the parent branch of $\tilde{\mathbf{b}}$, and $\mathcal{D}(\mathbf{b})$ represents child branches of $\mathbf{b}$. If the position of the bronchoscope is close to the bifurcation point ($\alpha < \gamma \left\|\tilde{\boldsymbol{b}}^e - \tilde{\boldsymbol{b}}^s\right\|$), the parent and sibling branches of $\tilde{\mathbf{b}}$ are selected for Φ. Otherwise, $\tilde{\mathbf{b}}$ is selected for Φ. Then, the inner product between ${}^{\mathrm{CT}}_{w}\mathbf{T}\boldsymbol{d}^k_w$ and the running direction of $\mathbf{b}_i = \left\{\boldsymbol{b}^s_i, \boldsymbol{b}^e_i\right\} \in \Phi$ is calculated. Finally, $\mathbf{b}_*$ is obtained as

$$\mathbf{b}_* = \arg\max_{\mathbf{b}_i \in \Phi} \frac{\left({}^{\mathrm{CT}}_{w}\mathbf{T}\boldsymbol{d}^k_w\right)\cdot\left(\boldsymbol{b}^e_i - \boldsymbol{b}^s_i\right)}{\left\|\boldsymbol{b}^e_i - \boldsymbol{b}^s_i\right\|}. \tag{6}$$

This chooses the branch whose running direction is most similar to the viewing direction of the bronchoscope camera.

Computation of corresponding point pairs

As seen in Fig. 3, $\boldsymbol{q}^k$ on the medial line of the bronchial branch $\mathbf{b}_*$ can be calculated as

$$\boldsymbol{q}^k = \boldsymbol{b}^s_* + \frac{\left({}^{\mathrm{CT}}_{w}\mathbf{T}\boldsymbol{p}^k_w - \boldsymbol{b}^s_*\right)\cdot\left(\boldsymbol{b}^e_* - \boldsymbol{b}^s_*\right)}{\left\|\boldsymbol{b}^e_* - \boldsymbol{b}^s_*\right\|}\frac{\left(\boldsymbol{b}^e_* - \boldsymbol{b}^s_*\right)}{\left\|\boldsymbol{b}^e_* - \boldsymbol{b}^s_*\right\|}, \tag{7}$$

where $\boldsymbol{q}^k$ is the foot of the perpendicular to the branch $\mathbf{b}_*$ that passes through ${}^{\mathrm{CT}}_{w}\mathbf{T}\boldsymbol{p}^k_w$. We denote a set of $\boldsymbol{q}^k$ as $\mathcal{Q} = \{\boldsymbol{q}^k\}$.

Estimation of the transformation matrix ${}^{\mathrm{CT}}_{w}\mathbf{T}$

We now utilize the radius r^k of the branch $\mathbf{b}_*$ for estimating the final transformation matrix. We denote a set of r^k as $\mathcal{R} = \{r^k\}$. Using $(\boldsymbol{p}^k_w, \boldsymbol{d}^k_w) \in \mathcal{P}, \boldsymbol{q}^k \in \mathcal{Q}$ and $r^k \in \mathcal{R}$, the transformation matrix ${}^{\mathrm{CT}}_{w}\mathbf{T}$ is estimated by minimizing

$$Err\left({}^{\mathrm{CT}}_{w}\mathbf{T}\right) = \sum_{\substack{(\boldsymbol{p}^k_w,\, \boldsymbol{d}^k_w) \in \mathcal{P},\\ \boldsymbol{q}^k \in \mathcal{Q},\ r^k \in \mathcal{R}}} \frac{\left\|\boldsymbol{q}^k - {}^{\mathrm{CT}}_{w}\mathbf{T}\boldsymbol{p}^k_w\right\|^2}{r^k}. \tag{8}$$

Powell's method [24] is used for minimizing this function.

Processes of sections "Selection of bronchial branches", "Computation of corresponding point pairs" and "Estimation of the transformation matrix ${}^{\mathrm{CT}}_{w}\mathbf{T}$" are repeated while Eq. (8) decreases.

An algorithm for estimating the matrix ${}^{\mathrm{CT}}_{w}\mathbf{T}$

The previous sections described the details of estimating the transformation matrix ${}^{\mathrm{CT}}_{w}\mathbf{T}$. Here, we summarize all required steps and formulate them as an algorithm.

The algorithm estimates ${}^{\mathrm{CT}}_{w}\mathbf{T}$ whenever N_1 outputs of the EMT sensor are obtained. Also, the estimation process will be started after N_2 outputs of the EMT sensor are obtained. The following algorithm uses j for representing the number of estimates of the transformation matrix ${}^{\mathrm{CT}}_{w}\mathbf{T}$, and ${}^{\mathrm{CT}}_{w}\mathbf{T}^j$ represents the transformation matrix obtained in the j-th estimation. Before applying the proposed algorithm, the bronchial branches $\mathbf{b}_i \in \mathcal{B}$ of a patient are extracted from the CT image using our previously developed method [22,23]. The complete algorithm follows.

Estimation of the transformation matrix ${}^{\mathrm{CT}}_{w}\mathbf{T}^j$

[**Step** 1] Initialize the transformation matrix ${}^{\mathrm{CT}}_{w}\mathbf{T}^0$ using an EMT sensor output when the bronchoscope camera is in the trachea.

[**Step** 2] Initialize each variable as $j \leftarrow 1$ and $\mathcal{P} \leftarrow \phi$.

[**Step** 3] According to the process described in section "Acquisition of bronchoscope positions and orientations by EMT", a set of bronchoscope camera positions and viewing directions is obtained as $\tilde{\mathcal{P}} = \{(\boldsymbol{p}^k_w, \boldsymbol{d}^k_w); k = 1, \ldots, N_1\}$, where $\boldsymbol{p}^k_w$ and $\boldsymbol{d}^k_w$ are the k-th position and viewing direction of the bronchoscope camera calculated from EMT sensor outputs. This acquisition is repeated until $\left|\tilde{\mathcal{P}}\right| \geq N_1$ is satisfied, where $\left|\tilde{\mathcal{P}}\right|$ is the number of elements included in the set $\tilde{\mathcal{P}}$. Then, $\mathcal{P}$ is updated as $\mathcal{P} \leftarrow \mathcal{P} \cup \tilde{\mathcal{P}}$.

[**Step** 4] If $|\mathcal{P}| < N_2$ is satisfied, return to **Step** 3.

[**Step** 5] Initialize a temporary transformation matrix $\mathbf{T}$ as $\mathbf{T} \leftarrow {}^{\mathrm{CT}}_{w}\mathbf{T}^{j-1}$.

[**Step** 6] For each $(\boldsymbol{p}^k_w, \boldsymbol{d}^k_w) \in \mathcal{P}, \boldsymbol{q}^k$ is calculated as follows. In the first step, a branch $\tilde{\mathbf{b}}$ is calculated using Eq. (4) with the matrix $\mathbf{T}$. Utilizing Eq. (2), this finds a branch $\tilde{\mathbf{b}}$ with minimum distance $D(\mathbf{T}\boldsymbol{p}^k_w, \mathbf{b}_i)$ to the bronchoscope camera among all bronchial branches $\mathbf{b}_i \in \mathcal{B}$. Then, $\mathbf{b}_*$ corresponding to $\mathbf{T}\boldsymbol{p}^k_w$ is obtained by Eqs. (5) and (6), and $\boldsymbol{q}^k \in \mathcal{Q}$ is calculated using Eq. (7). Also, the radius $r^k \in \mathcal{R}$ of the branch $\mathbf{b}_*$ is calculated from the previously extracted bronchial tree structure.

[**Step** 7] Using $(\boldsymbol{p}^k_w, \boldsymbol{d}^k_w) \in \mathcal{P}, \boldsymbol{q}^k \in \mathcal{Q}, \boldsymbol{r}^k \in \mathcal{R}$ obtained in **Step** 6, the transformation matrix $\mathbf{T}'$ is calculated by minimizing Eq. (8). Here, the transformation matrix $\mathbf{T}$ is used as the initial estimate of this minimization step.

[**Step** 8] $Err(\mathbf{T})$ and $Err(\mathbf{T}')$ are calculated using Eq. (8). If $Err(\mathbf{T}') < Err(\mathbf{T})$ is satisfied, update the matrix $\mathbf{T}$ as $\mathbf{T} \leftarrow \mathbf{T}'$ and then return to **Step** 6. Otherwise, move to the next step.

[**Step** 9] ${}^{\mathrm{CT}}_{w}\mathbf{T}^j \leftarrow \mathbf{T}$

[**Step** 10] $j \leftarrow j + 1$.

[**Step** 11] Return to **Step** 3.

Experimental results

In the experiments carried out in this paper, we used a rubber bronchial phantom shown in Fig. 4. The rubber bronchial phantom was fixed in epoxy resin inside a plastic box whose size was 200 mm × 200 mm × 200 mm, and 18 acrylic pipes

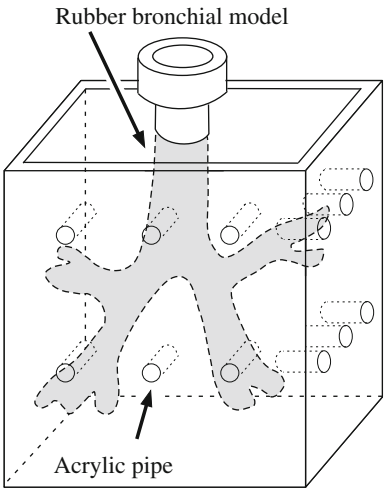

Fig. 4 Rubber bronchial phantom used in our experiments. The rubber bronchial phantom was fixed in epoxy resin inside a plastic box, and 18 acrylic pipes (2 mm diameter) were drilled into the box

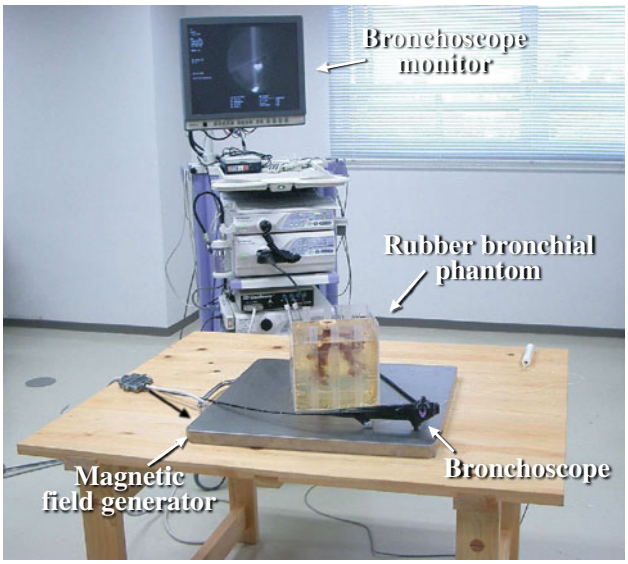

Fig. 5 Experimental environment

(2 mm diameter) were drilled into the box. Then, a 3D CT image of this phantom was taken by a multi-detector CT device (Aquillion 16, Toshiba Medical Systems Inc., Tokyo). The acquisition parameters of the CT image were 512 × 512 pixels, 341 slices, 0.684 mm in pixel spacing, and 0.5 mm in image spacing. All experiments were carried out using a BF-260 type bronchoscope (Olympus Inc., Tokyo), and we used a 3D Guidance tracking system (Ascension Technology Inc., VT) for EMT. The latter consists of two parts: (a) a flat type magnetic field generator and (b) a sensing coil. The sensing coil is 1.3 mm in diameter and 6.7 mm in length. Therefore, we could insert the EMT sensor into the working channel of the bronchoscope and fix it at the tip of the bronchoscope. Since the tracking system can sense a volume of 460 mm × 460 mm × 460 mm, it covers enough area for bronchoscopy and provides six degrees of freedom (three each for rotation and translation). The proposed method was tested on a Dell Precision Workstation 490 (CPU: Intel Quad Core Xeon 3.0 GHz×2, 4 GB RAM). As shown in Fig. 5, the environment has no metal materials within one meter of the magnetic field generator, and the magnetic field generator was placed on a purely wooden table. The phantom was placed about 250 mm above the magnetic field generator, and the distance between the magnetic field generator and the PC was greater than 2 m.

${}^{\mathrm{CT}}_{w}\mathbf{T}^{j}$ was estimated by inserting the bronchoscope camera into several bronchial branches of the phantom. Two thousand pairs of EMT sensor outputs and bronchoscopic images (10 samples per second) were obtained by inserting the bronchoscope camera in the following orders: trachea → right main bronchus → left main bronchus → left lower lobe bronchus → left upper lobe bronchus → right upper lobe bronchus → right lower lobe bronchus. This insertion path was determined based on the suggestions from a medical doctor. We used $N_1 = 20$, $N_2 = 200$ and $\gamma = 0.2$ for estimating the transformation matrix ${}^{\mathrm{CT}}_{w}\mathbf{T}^{j}$. Since the phantom does not move during the experiments, we assumed the transformation matrix ${}^{w}_{F}\mathbf{T}$ to be the identity matrix. After fixing the EMT sensor at the tip of the bronchoscope camera, we manually adjusted the transformation matrix ${}^{s}_{c}\mathbf{T}$ representing the relationship between the bronchoscope camera and the EMT sensor. This step however could be automated by applying hand–eye calibration [20], or by applying the method based on a calibration chart [21]. According to the suggestion of a medical doctor, we initialized ${}^{\mathrm{CT}}_{w}\mathbf{T}^{0}$ using an EMT sensor output when the bronchoscope camera was located inside the trachea. This is because doctors always keep the bronchoscope camera in the same orientation inside the trachea to compare their knowledge and the patient's bronchial structure. Figure 6 shows virtual bronchoscopic images generated inside three different airway branches when increasing the number of j.

To evaluate the efficiency of the proposed method, we compare it with our previously published method [16] that does not use the stable branch selection mechanism described in section "Selection of bronchial branches". In this experiment, the tips of 18 acrylic pipes fixed in the box were used for evaluating the accuracy of ${}^{\mathrm{CT}}_{w}\mathbf{T}^{j}$ estimated by the previous method and the proposed method. Gold standards for computing the error were obtained by conducting the following two steps. First, the EMT sensor was manually inserted and fixed at each tip of the acrylic pipes, and then the tip positions $\boldsymbol{p}^{k}_{w}$ $(k = 1, \ldots, 18)$ were computed from the outputs of the EMT sensor. Next, the points $\boldsymbol{p}^{k}_{\mathrm{CT}}(k = 1, \ldots, 18)$ corresponding to $\boldsymbol{p}^{k}_{w}$ were manually identified in the CT image. Finally, the error was computed as

$$Err^{j} = \frac{1}{18}\sum_{k=1}^{18}\left\| \boldsymbol{p}^{k}_{\mathrm{CT}} - {}^{\mathrm{CT}}_{w}\mathbf{T}^{j}\,\boldsymbol{p}^{k}_{w} \right\| \tag{9}$$

Here, each $\boldsymbol{p}^{k}_{w}(k = 1, \ldots, 18)$ was obtained by taking the average of 100 measurements. We evaluated Eq. (9) of the previous method and the proposed method (Fig. 7). Figure 8 shows the computation time of the previous method and the proposed method for estimating ${}^{\mathrm{CT}}_{w}\mathbf{T}^{j}$. Figure 9 shows EMT sensor outputs and the bronchial tree structure used for estimating the transformation matrix ${}^{\mathrm{CT}}_{w}\mathbf{T}^{j}$. The points shown in Fig. 9 are calculated by applying the transformation matrix ${}^{\mathrm{CT}}_{w}\mathbf{T}^{j}$ to the EMT sensor outputs.

To evaluate the robustness of the previous method and the proposed method against breathing motion, we also estimated the transformation matrix ${}^{\mathrm{CT}}_{w}\mathbf{T}^{j}$ when adding virtual breathing motion to the EMT sensor outputs. We used a simple approximation of [25] for virtual breathing motion, and the displacement was added to EMT outputs so that it was

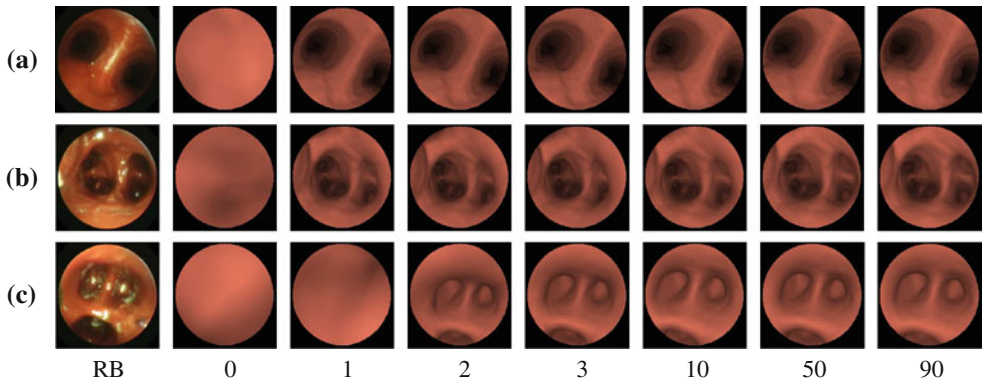

Fig. 6 Virtual bronchoscopic images generated using the transformation matrix ${}^{\mathrm{CT}}_{w}\mathbf{T}^{j}$ when changing the number of estimates j. **a** trachea, **b** right lower lobe bronchus, and **c** left lower lobe bronchus

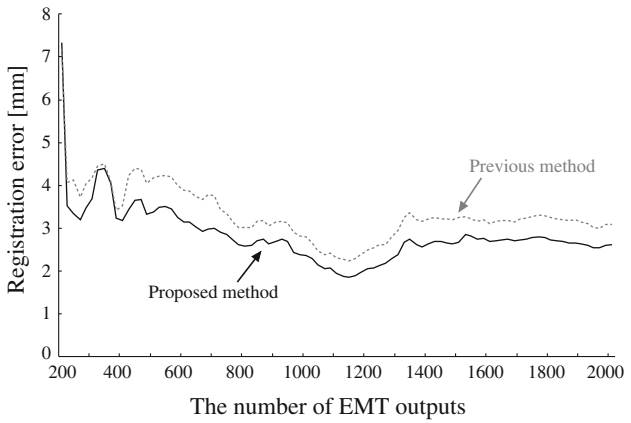

Fig. 7 Error of ${}^{\mathrm{CT}}_{w}\mathbf{T}^{j}$ without virtual breathing motion

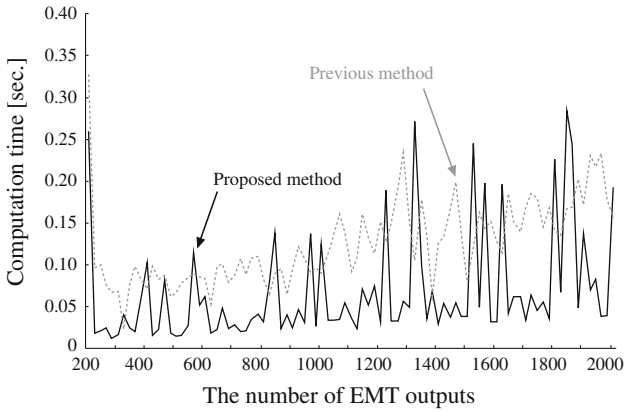

Fig. 8 Computation time of ${}^{\mathrm{CT}}_{w}\mathbf{T}^{j}$ without virtual breathing motion

linearly interpolated between the carina and the diaphragm. Concretely, the breathing motion was simply approximated as linear motion along the direction from carina to diaphragm. And, the displacement of EMT outputs was determined so that it was proportional to the distance from carina and took maximum at diaphragm. We defined the parameters of the virtual breathing motion as follows.

- Breathing cycle: 6 s
- Displacement of the diaphragm: $\pm$ 20 mm

By applying this virtual breathing motion, the displacement of the right and the left lower lobe bronchi was about $\pm$ 15 mm. Figure 10 shows the error of the previous and the proposed methods when adding the breathing motion to the EMT sensor outputs. Figure 11 shows the computation time

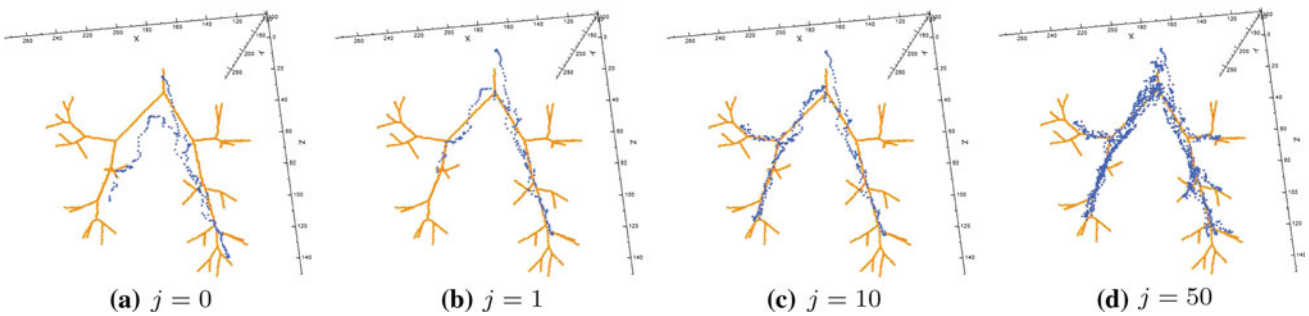

Fig. 9 Bronchoscope camera positions calculated from EMT sensor outputs and the transformation matrix ${}^{\mathrm{CT}}_{w}\mathbf{T}^{j}$ when changing the number of estimates j

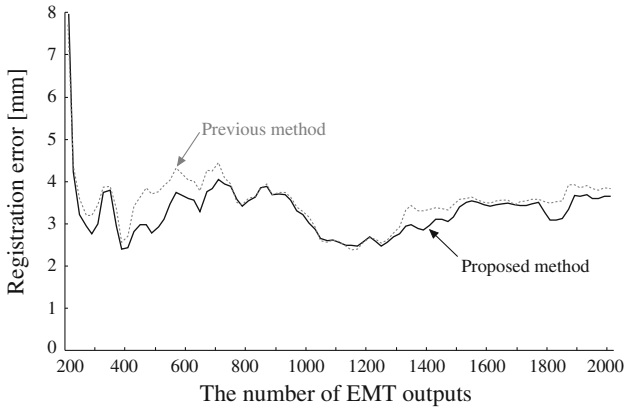

Fig. 10 Error of ${}^{\mathrm{CT}}_{w}\mathbf{T}^{j}$ with virtual breathing motion

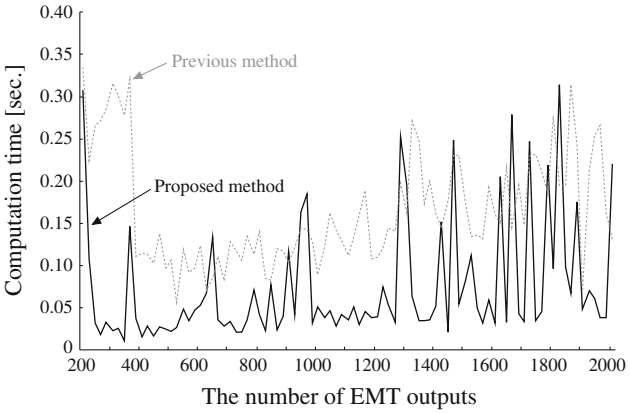

Fig. 11 Computation time of ${}^{\mathrm{CT}}_{w}\mathbf{T}^{j}$ with virtual breathing motion

of both methods, Fig. 12 shows EMT sensor outputs obtained by applying the estimated transformation matrix ${}^{\mathrm{CT}}_{w}\mathbf{T}^{j}$.

Discussion

As shown in Fig. 7, it can be confirmed that the error of both the previous method and the proposed method tends to decrease when increasing the number of EMT sensor outputs. When comparing the number of estimates j required to obtain an error smaller than 3 mm, the previous method required $j = 39$(960 EMT outputs) and the proposed method required $j = 27$(720 EMT outputs). These results indicate that the proposed method can estimate a more accurate transformation matrix using a smaller number of estimates than the previous method. The accuracy of our method is better than that in [12]. While [12] requires fiducial markers or natural landmarks to perform registration, our proposed method requires no fiducial marker or the like. Our marker-free registration algorithm can reduce the initialization time of a bronchoscopic guidance system. This is a great advantage over methods that utilize fiducial markers or natural landmarks.

As seen in Fig. 7, our proposed method requires only 0.065 s (SD: 0.065) for estimating the transformation matrix, while our previously proposed method requires 0.125 s (SD: 0.050). This is also faster than the method by Klein et al. [15] which took about 2–5 min. Therefore, our proposed method can improve both the accuracy and the computation time in comparison with the previous methods.

Although the proposed method assumes the bronchoscope camera moves along the medial line of the airways or close to the center of the airway lumen, this may not always be satisfied due to hand movement or hand shaking. However, as seen in Figs. 9 and 12, if we insert the bronchoscope camera several times into the airways, it can be observed that the positions of the bronchoscope camera are distributed around the medial line of the airways. Therefore, the proposed method could decrease the error of the transformation matrix by increasing the number of EMT sensor outputs.

When the bronchoscope camera is close to a bifurcation point of the bronchus, there is an ambiguity in the correspondences between an EMT sensor output and bronchial branches, because distances between them are almost the same. Since the previous method calculated correspondences by evaluating the minimum distance only, the error of the transformation matrix ${}^{\mathrm{CT}}_{w}\mathbf{T}\boldsymbol{p}^{k}_{w}$ was increased in such cases. In contrast, our proposed method tries to reduce such an

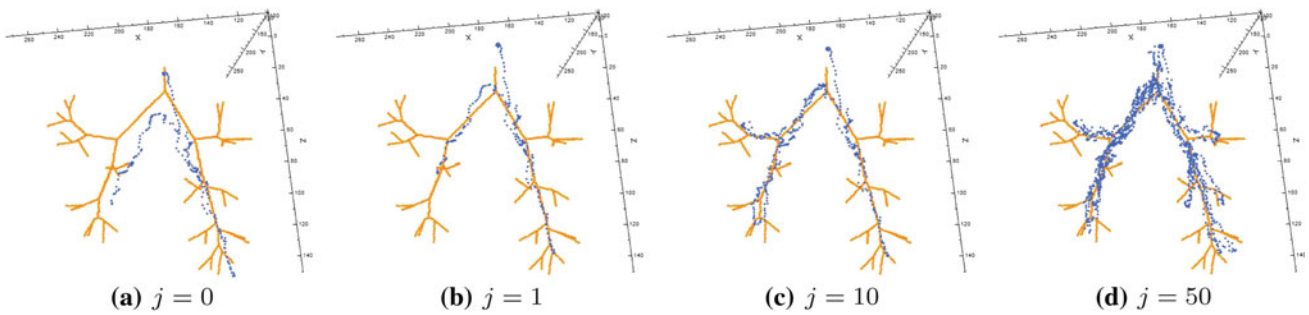

Fig. 12 Bronchoscope camera positions calculated from EMT sensor outputs and the transformation matrix ${}^{\mathrm{CT}}_{w}\mathbf{T}^{j}$ when changing the number of estimates j. Virtual breathing motion was added to the EMT sensor outputs

error by evaluating the difference between the viewing direction of the bronchoscope camera and the running direction of bronchial branches. Also, the proposed method uses the radius of each bronchial branch for distance calculation in Eq. (8) in order to normalize differences between branches. Using these approaches, the proposed method can improve the accuracy compared with the previous method, as shown in Fig. 7.

As seen in Fig. 10, the accuracy of our proposed method is within about 3.5 mm even if virtual breathing motion was added to the EMT sensor outputs. This is much smaller than the displacement of EMT sensor outputs caused by virtual breathing motion. The computation time of our proposed method under virtual breathing was 0.074 s (SD: 0.072). From these results, we can see that the proposed method can estimate the transformation matrix even if EMT sensor outputs are affected by breathing motion. Although the proposed method obtained little improvement regarding the error, the computation time was greatly reduced in comparison with the previous method. However, since the proposed method uses a rigid transformation matrix for registering the coordinate systems of the CT and the patient, the error may be increased when the deformation of the airways is larger than in our simulations. In the case of a real patient, the breathing motion becomes much complicated, especially in a diseased lung. Therefore, the proposed method should be extended to estimate a non-rigid transformation and should be evaluated by real breathing motion. Also, it is necessary to develop a method to compensate the difference between movements of the DRF and the lung. These should be solved as our future work.

In this experiment, the transformation matrix ${}^{s}_{c}\mathbf{T}$ was calculated using the specifications of the bronchoscope (the placement of the camera and the working channel) and the EMT sensor, and then adjusted manually so that real bronchoscopic images resembled the virtual bronchoscopic images generated using the transformation matrix. Since the diameter of the bronchoscope's tip is small enough, the EMT sensor could be attached close to the camera. Therefore, we assumed that the error caused by the transformation matrix ${}^{s}_{c}\mathbf{T}$ can be ignored. However, we should evaluate the influence of the transformation matrix ${}^{s}_{c}\mathbf{T}$ in our future work.

Conclusions

This paper presented a method for automated CT-to-patient registration using a position sensor without fiducial markers and natural landmarks. The proposed method segments the airways from a CT image taken prior to bronchoscopy. Then, the transformation matrix ${}^{\mathrm{CT}}_{w}\mathbf{T}$ between the coordinate systems of the patient and the CT image is calculated using EMT sensor outputs and the bronchial tree structure. To improve the robustness of the transformation matrix estimation, the proposed method introduces a stable bronchial branch selection mechanism. Experimental results showed that the proposed method could estimate the transformation matrix within an accuracy of about 3.0 mm. Moreover, the proposed method could estimate the transformation matrix even if the EMT sensor outputs were affected by breathing motion. Future work includes: (i) in-vivo experiments and (ii) extension of the registration to a non-rigid case.

Acknowledgments The authors would like to thank our colleagues for their useful suggestions and enlightening discussions. Parts of this research were supported by a Grant-In-Aid for Scientific Research from the Ministry of Education, a Grant-In-Aid for Scientific Research from the Japan Society for Promotion of Science, a Grant-In-Aid for Cancer Research from the Ministry of Health and Welfare of the Japanese Government, the program of the formation of innovation center for fusion of advanced technologies funded by the MEXT, and JSPS postdoctoral fellowship program for foreign researchers.

Conflict of interest None.

References

1. Vining DJ, Shitrin RY, Haponik EF, Liu K, Choplin RH (1994) Virtual bronchoscopy. Radiology, vol 193(P), Supplement to radiology (RSNA Scientific Program), p 261
2. Geiger B, Kikinis R (1995) Simulation of endoscopy, Computer vision, virtual reality and robotics in medicine, LNCS 905. Springer, pp 277–281
3. Rubin G, Beaulieu C, Argiro V, Ringl H, Norbash A, Feller J, Dake M, Jeffrey R, Napel S (1996) Perspective volume rendering of CT and MR images: applications for endoscopic imaging. Radiology 199: 321–330
4. Mori K, Urano A, Hasegawa J, Toriwaki J, Anno H, Katada K (1996) Virtualized endoscope system—an application of virtual reality technology to diagnostic aid. IEICE Trans Inf Syst E79–D(6): 809–819
5. Hong L, Muraki S, Kaufman A, Bartz D, He T (1997) Virtual voyage: interactive navigation in the human colon. In: Proceedings of the 24th annual conference on computer graphics and interactive techniques (SIGGRAPH'97), pp 27–34
6. Rogalla P, Terwisschavan Scheltinga J, Hamm B (eds) (2001) Virtual endoscopy and related 3D techniques. Springer, Berlin
7. Caramella D, Bartolozzi C (eds) (2002) 3D image processing — techniques and clinical application. Springer, Berlin
8. Bricault I, Ferretti G, Cinquin P (1998) Registration of real and CT-derived virtual bronchoscopic images to assist transbronchial biopsy. IEEE Trans Med Imaging 17(5):703–714
9. Helferty JP, Higgins WE (2001) Technique for registering 3D virtual CT images to endoscopic video. In: Proceedings of international conference on image processing (ICIP2001), pp 893–896
10. Merritt SA, Rai L, Higgins WE (2006) Real-time CT-video registration for continuous endoscopic guidance. In: Proceedings of SPIE medical imaging, vol 6143, pp 614313-1–614313-15
11. Mori K, Deguchi D, Sugiyama J, Suenaga Y, Toriwaki J, Maurer CR Jr, Takabatake H, Natori H (2002) Tracking of a bronchoscope using epipolar geometry analysis and intensity-based image registration of real and virtual endoscopic images. Med Image Anal 6:321–336

12. Schneider A, Hautmann H, Barfuss H, Pinkau T, Peltz F, Feussner H, Wichert A (2004) Real-time image tracking of a flexible bronchoscope. In: Proceedings of CARS2004, vol 1268, pp 753–757
13. Deligianni F, Chung AJ, Yang GZ (2006) Nonrigid 2-D/3-D registration for patient specific bronchoscopy simulation with statistical shape modeling: phantom validation. IEEE Trans Med Imaging 25(11):1462–1471
14. Wegner I, Biederer J, Tetzlaff R, Wolf I, Meinzer H (2007) Evaluation and extension of a navigation system for bronchoscopy inside human lungs. In: Proceedings of SPIE medical imaging 2007, vol 6509, pp 65091H-1–65091H-12
15. Klein T, Traub J, Hautmann H, Ahmadian A, Navab N (2007) Fiducial-free registration procedure for navigated bronchoscopy. In: Proceedings of the 10th international conference on medical image computing and computer assisted intervention (MICCAI2007), Part I, LNCS, vol 4791, pp 475–482
16. Deguchi D, Ishitani K, Kitasaka T, Mori K, Suenaga Y, Takabatake H, Mori M, Natori H (2007) A method for bronchoscope tracking using position sensor without fiducial markers. In: Proceedings of SPIE medical imaging 2007, vol 6511, pp 65110N-1–65110N-12
17. Mori K, Deguchi D, Ishitani K, Kitasaka T, Suenaga Y, Hasegawa Y, Imaizumi K, Takabatake H (2007) Bronchoscope tracking without fiducial markers using ultra-tiny electromagnetic tracking system and its evaluation in different environments. In: Proceedings of the 10th international conference on medical image computing and computer assisted intervention (MICCAI2007), Part II, LNCS vol 4792, pp 644–651
18. Mori K, Deguchi D, Kitasaka T, Suenaga Y, Hasegawa Y, Imaizumi K, Takabatake H (2008) Improvement of accuracy of marker-free bronchoscope tracking using electromagnetic tracker based on bronchial branch information. In: Proceedings of the 11th international conference on medical image computing and computer assisted intervention (MICCAI2008), Part II, LNCS, vol 5242, pp 535–542
19. Besl PJ, McKay HD (1992) A method for registration of 3-D shapes. IEEE Trans Pattern Anal Mach Intell 14(2):239–256
20. Tsai RY, Lenz RK (1988) Real time versatile robotics hand/eye calibration using 3D machine vision. In: Proceedings of 1988 IEEE international conference on robotics and automation, pp 554–561
21. Shahidi R, Bax MR, Maurer CR Jr, Johnson JA, Wilkinson EP, Wang B, West JB, Citardi MJ, Manwaring KH, Khadem R (2002) Implementation, calibration and accuracy testing of an image-enhanced endoscopy system. IEEE Trans Med Imaging 21(12): 1524–1535
22. Kitasaka T, Mori K, Hasegawa J, Toriwaki J (2002) A method for extraction of bronchus regions from 3D chest X-ray CT images by analyzing structural features of the bronchus. FORMA 17(4): 321–338
23. Feuerstein M, Kitasaka T, Mori K (2009) Adaptive branch tracing and image sharpening for airway tree extraction in 3-D chest CT. In: Proceedings of second international workshop on pulmonary image analysis, pp 273–284
24. Press WH, Teukolsky SA, Vetterling WT, Flannery BP (1999) Numerical recipes in C, the art of scientific computing second edition. Cambridge University Press, Cambridge, pp 321–336
25. Soper TD, Haynora DR, Glenny RW, Seibela EJ (2007) A model of respiratory airway motion for real-time tracking of an ultra-thin bronchoscope. In: Proceedings of SPIE medical imaging 2007, vol 6511, pp 65110M-1–65110M-12